Environ Geol (2007) 52:615–623
DOI 10.1007/s00254-006-0491-y

ORIGINAL ARTICLE

Application and verification of fuzzy algebraic operators to landslide susceptibility mapping

Saro Lee

Received: 12 June 2006 / Accepted: 28 August 2006 / Published online: 20 September 2006

Abstract The aim of this study was to apply and to verify the use of fuzzy logic to landslide susceptibility mapping in the Gangneung area, Korea, using a geographic information system (GIS). For this aim, in the study, a data-derived model (frequency ratio) and a knowledge-derived model (fuzzy operator) were combined. Landslide locations were identified by changing the detection technique of KOMPSAT-1 images and checked by field studies. For landslide susceptibility mapping, maps of the topography, lineaments, soil, forest, and land cover were extracted from the spatial data sets, and the eight factors influencing landslide occurrence were obtained from the database. Using the factors and the identified landslide, the fuzzy membership values were calculated. Then fuzzy algebraic operators were applied to the fuzzy membership values for landslide susceptibility mapping. Finally, the produced map was verified by comparing with existing landslide locations for calculating prediction accuracy. Among the fuzzy operators, in the case in which the gamma operator ($\lambda = 0.975$) showed the best accuracy (84.68%) while the case in which the fuzzy or operator was applied showed the worst accuracy (66.50%).

Keywords Landslide · GIS · Fuzzy operator · Fuzzy membership function · Frequency ratio · Korea

S. Lee (✉)
Geoscience Information Center, Korea Institute of Geoscience & Mineral Resources (KIGAM), 30, Gajeong-dong, Yuseong-gu, Daejeon 305-350, South Korea
e-mail: leesaro@kigam.re.kr

Introduction

Landslides are one of the major natural geological hazards, and every year they are responsible for enormous property damage and both direct and indirect costs. Korea experiences frequent landslides, with the most recent ones occurring in 1996, 1998, 1999, and 2002. They often result in significant damage to people and property. From 20 to 31 August, typhoon Rusa has hit the Gangneung area in the form of heavy rainfall and storm. The daily total rainfall was 609 mm and hourly rainfall was 80 mm. Two hundred and sixty six people died and the damage to property caused by this typhoon was about US$ 8 billion. Among these, 81 people died by landslide and collapse of cut-slope. The Gangneug area was selected because it is one of the areas most vulnerable to landslides. This region (Fig. 1) lies between the 36°25′N and 36°30′N, and 127°40′E and 127°45′E, and covers an area of 68 km^2. The main lithological unit of the study area is formed by granites.

The landslides in Gangneung, which were triggered by the heavy rainfall, caused extensive damage as there had been little effort to assess or predict the event. Scientific analysis of landslides enables us to assess landslide-susceptible areas and thereby to predict landslide and reduce landslide damage. In order to achieve this, a landslide-susceptibility analysis technique was introduced, applied, and verified using fuzzy algebraic operators. Landslide locations were identified by the change detection technique of KOMPSAT-1 images and checked in field (Fig. 1). For landslide susceptibility mapping, maps of the topography, lineaments, soil, forest, and land cover were constructed from the spatial data sets. Then, the eight factors

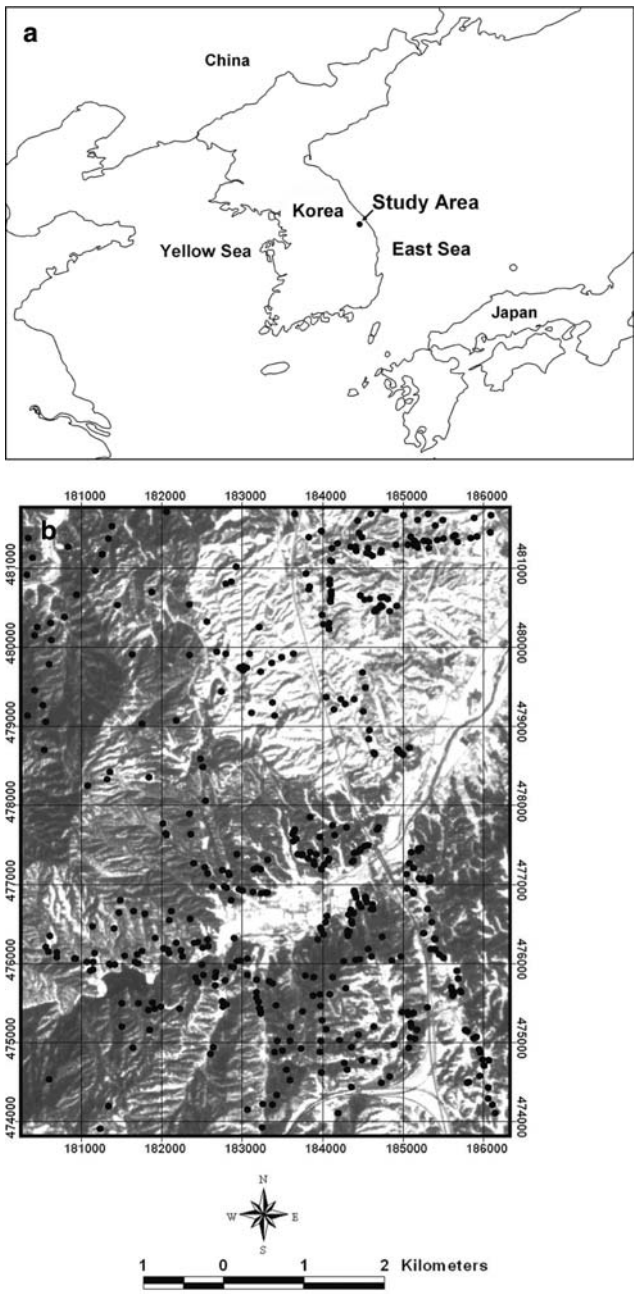

Fig. 1 The study area (**a**) and KOMPSAT 1 images with landslide locations (**b**)

affecting landslide occurrence were extracted from the database. Using the factors and the detected landslide, the relationships were calculated using the frequency ratio, one of the probabilistic models. Then, the fuzzy membership values were also calculated using the frequency ratio. The fuzzy membership values were combined using the fuzzy and, fuzzy or, fuzzy algebraic product, fuzzy algebraic sum, and fuzzy gamma operators (13 cases) for landslide susceptibility mapping. Finally, the map was verified by comparing with existing landslide locations for calculating prediction accuracy.

Many studies have been carried out on landslide hazard evaluation using GIS; for example, Guzzetti et al. (1999) summarized many landslide hazard evaluation studies. Recently, there have been studies on landslide hazard evaluation using GIS, and many of these studies have applied probabilistic models (Jibson et al. 2000; Luzi et al. 2000; Parise and Jibson 2000; Baeza and Corominas 2001; Lee and Min 2001; Clerici et al. 2002; Donati and Turrini 2002; Lee et al. 2002a, b, 2004b, c; Zhou et al. 2002; Lee and Choi 2003, 2004). One of the available statistical models, the logistic regression models, has also been applied to landslide hazard mapping (Atkinson and Massari 1998; Dai et al. 2001; Dai and Lee 2002; Ohlmacher and Davis 2003; Lee 2004), as has the geotechnical model and the safety factor model (Gokceoglu et al. 2000; Romeo 2000; Refice and Capolongo 2002; Carro et al. 2003; Shou and Wang 2003; Zhou et al. 2003). As a new approach to landslide hazard evaluation using GIS, data mining using fuzzy logic, and artificial neural network models have been applied (Ercanoglu and Gokceoglu 2002; Pistocchi et al. 2002; Lee et al. 2003a, b, 2004a; Ercanoglu and Gokceoglu 2004).

Data

To apply the fuzzy approach, a spatial database considering landslide-related factors, such as topography, soil, forest, geology, lineament, and land cover, was used. These thematic maps (topography, soil, forest and geology, for example) are available in Korea in either paper or digital form. The lineament and land cover were detected from satellite images such as IRS (Indian Remote Sensing) and Landsat TM (Thematic Mapper) images. The spatial database is shown in Table 1. The landslide map is in the form of point coverage, the topographic map in the form of line and point coverage at a scale of 1:5,000, the geological map in the form of polygon coverage at a scale of 1:50,000, the soil map in the form of polygon coverage at a scale of 1:25,000, the forest map in the form of polygon coverage at a scale of 1:25,000, the lineament map in the form of line coverage, and the land cover in grid form with a resolution of 5 m. The thematic maps employed in the present study were made by national organizations such as The National Geographic Institute for the topographic map, The Korea Institute of Geoscience and Mineral Resources for the geological map, The National Institute of Agricultural Science

Table 1 Type and scale of the data used in the study

Classification	Subclassification	Data type	Scale
Geological hazard	Landslide	Point coverage	1:5,000
Basic map	Topographic map	Line and point coverage	1:5,000
	Geological map	Polygon coverage	1:50,000
	Lineament map	Line coverage	1:50,000
	Drainage network map	Line coverage	1:5,000
	Soil map	Polygon coverage	1:25,000
	Forest map	Polygon coverage	1:25,000
Image data	Landsat TM	Image	30 m × 30 m
	Land use	GRID	5 m × 5 m
	KOMPSAT satellite image	Image	6.6 m × 6.6 m

and Technology for the soil map, and The National Forest Research Institute for the forest map.

Eight factors, extracted from the constructed spatial database, were considered when calculating the probability. Contour and survey base points that have an elevation value were extracted from the topographic map and triangulated irregular network (TIN) was made using the elevation value. A digital elevation model (DEM) was made using the inverse distance weighting (IDW) interpolation method with 5 m resolution. The slope angle, slope aspect, and slope curvature were obtained from the DEM. The distance from drainage network was calculated at 1-m intervals using the one topographic map. The soil type was acquired from a soil map and the timber type was obtained from a forest map. The lithology map was obtained from a geologic map, but because the lithology of the study area is of the same type, granite, it was excluded from the analysis. The lineament was detected from interpretation of the IRS panchromatic image. A structural geologist interpreted the IRS image by photointerpretation and detected the lineaments. The distance from lineament was then calculated at 1-m intervals. Finally, landuse data was classified from a LANDSAT TM image using the unsupervised (ISODATA) classification method. The six remaining classes, such as urban land, water, forest, agricultural and barren areas, were extracted for land cover mapping. Overall, the Gangneung data set comprised 1,586 rows by 1,209 columns, with a total cell number of 1,917,474. Landslides had occurred in 107 of these cells.

Methodology

The fuzzy set theory introduced by Zadeh (1965) is one of the tools used to handle the complex problems. Therefore, the fuzzy set theory has been commonly used for many scientific studies in different disciplines. The idea of fuzzy logic is to consider the spatial objects on a map as members of a set. In the classical set theory, an object is a member of a set if it has a membership value of 1, or is not a member if it has a membership value of 0. In the fuzzy set theory, membership can take on any value between 0 and 1 reflecting the degree of certainty of membership. The fuzzy set theory employs the idea of a membership function that expresses the degree of membership with respect to some attribute of interest.

With maps, generally, the attribute of interest is measured over discrete intervals, and the membership function can be expressed as a table relating map classes to membership values. Fuzzy logic is attractive because it is straightforward to understand and implement. It can be used with data from any measurement scale and the weighting of evidence is controlled entirely by the expert. The fuzzy logic method allows for more flexible combinations of weighted maps, and could be readily implemented with a GIS modeling language. This is different from data-driven approaches such as weights of evidence or logistic regression, which use the locations of known objects such as landslides to estimate weights or coefficients. The idea of using fuzzy logic in landslide susceptibility mapping is to consider the spatial objects on a map as members of a set. For example, the spatial objects could be areas on an evidence map and the set defined as 'areas susceptible to landslide'. Fuzzy membership values must lie in the range (0, 1), but there are no practical constraints on the choice of the fuzzy membership values. Values are chosen to reflect the degree of membership of a set, based on subjective judgment. Given two or more maps with fuzzy membership functions for the same set, a variety of operators can be employed to combine the membership values.

Zimmerman (1996) discussed a variety of combination rules. Bonham-Carter (1994) discussed five operators, namely the fuzzy and, fuzzy or, fuzzy algebraic product, fuzzy algebraic sum, and fuzzy gamma operator. This study uses the five fuzzy operators for combining the fuzzy membership functions.

The fuzzy and is equivalent to a Boolean AND (logical intersection) operation on classical set values of Eq. 1. It is defined as

$$\mu_{\text{combination}} = \text{MIN}(\mu_A, \mu_B, \mu_C, \ldots), \quad (1)$$

where $\mu_{\text{combination}}$ is the calculated fuzzy membership function, μ_A is the membership value for map A at a particular location, and μ_B is the value for map B, and so on.

The fuzzy or is like the Boolean OR (logical union in that the output membership values are controlled by the maximum values of any of the input maps). The fuzzy or is defined as:

$$\mu_{\text{combination}} = \text{MAX}(\mu_A, \mu_B, \mu_C, \ldots). \quad (2)$$

The fuzzy algebraic product is defined as:

$$\mu_{\text{combination}} = \prod_{i=1}^{n} \mu_i, \quad (3)$$

where μ_i is the fuzzy membership function for the ith map, and $i = 1, 2, ..., n$ maps are to be combined.

The fuzzy algebraic sum is complementary to the fuzzy algebraic product, being defined as

$$\mu_{\text{combination}} = 1 - \prod_{i=1}^{n} (1 - \mu_i). \quad (4)$$

The gamma operation is defined in terms of the fuzzy algebraic product and the fuzzy algebraic sum by

$$\mu_{\text{combination}} = (\text{Fuzzy algebraic sum})^{\lambda} * (\text{Fuzzy algebraic product})^{1-\lambda}, \quad (5)$$

where λ is a parameter chosen in the range (0,1), and the fuzzy algebraic sum and fuzzy algebraic product are calculated using Eqs. 3 and 4, respectively. In the fuzzy gamma operation, when λ is 1 the combination is the same as the fuzzy algebraic sum, and when λ is 0 the combination equals the fuzzy algebraic product. Judicious choice of λ produces output values that ensure a flexible compromise between the 'increase' tendencies of the fuzzy algebraic sum and the 'decrease' effects of the fuzzy algebraic product.

Like the membership function, the frequency ratio was calculated. The frequency ratio is shown in Table 2 for all factors. The spatial relationships between the landslide location and each landslide-related factor were analyzed by using the probability model–frequency ratio. The frequency ratio, a ratio between the occurrence and absence of landslides in each cell, was calculated for each factor's type or range that had been identified as significant with respect to causing landslides. An area ratio for each factor's type or range to the total area was calculated. Finally, frequency ratios for each factor's type or range were calculated by dividing the landslide occurrence ratio by the area ratio. If the ratio is greater than 1, the relationship between landslides and the factors is higher and, if the ratio is less than 1, the relationship between landslide and each factor's type or range is lower. Then, the frequency ratio was normalized between 0.00 and 1.00 to create the fuzzy membership value.

Application and verification of fuzzy logic to landslide susceptibility mapping

The input factors were combined for assigning membership functions. Eight landslide causal factors (slope, aspect, curvature, distance from drainage, soil, forest, distance from fault, and land cover) were combined to generate the final susceptibility map using fuzzy operators such as fuzzy and, fuzzy or, fuzzy algebraic product, fuzzy algebraic sum, and fuzzy gamma operator. In the case of fuzzy gamma operator, the value of λ was set to 0.025, 0.05, 0.1, 0.2, 0.3, 0.4, 0.5, 0.6, 0.7, 0.8, 0.9, 0.95, and 0.975 to detect its effect on the landslide susceptibility map.

Using the fuzzy membership function (Table 2) and the fuzzy operator (from Eqs. 1 to 5), the landslide susceptibility index (LSI) values were computed for the 17 cases including the 13 cases in which the gamma operator was used. The computed LSI values were mapped to allow interpretation such as that illustrated, for example, in Fig. 2. The values were classified into equal areas and grouped into five classes for visual interpretation. For example, in the case of applying the fuzzy algebraic product, the minimum, mean, maximum, and standard deviation values of each LSI are 0.00, 0.000918, 0.207196, and 0.003045, respectively. In the case of applying the fuzzy algebraic sum, the minimum, mean, maximum, and standard deviation values of each LSI are 0.802456, 0.996293, 1.000000, and 0.006898, respectively. In the case of applying the gamma operator ($\lambda = 0.975$), the minimum, mean, maximum, and standard deviation values of each LSI are 0.4496, 0.7663, 0.9614, and 0.0731, respectively. Also, in the case of applying the gamma operator ($\lambda = 0.025$), the minimum, mean, maximum, and standard deviation values of each LSI are 0.00, 0.067847, 0.215512, and 0.003354, respectively.

Table 2 Spatial relationships between each factor and landslide and fuzzy membership values

Factor	Class	No. of pixels in domain	Percentage of domain	No. of landslide	Percentage of landslide	Frequency ratio	Fuzzy membership values
Slope	0–5	336,945	17.57	0	0.00	0.00	0.00
	6–10	204,758	10.68	2	0.59	0.06	0.01
	11–15	311,658	16.25	13	3.86	0.24	0.04
	16–20	362,062	18.88	46	13.65	0.72	0.13
	21–25	322,133	16.80	78	23.15	1.38	0.24
	26–30	217,740	11.36	97	28.78	2.53	0.44
	31–35	108,568	5.66	67	19.88	3.51	0.61
	36–40	39,827	2.08	20	5.93	2.86	0.49
	41–90	13,783	0.72	14	4.15	5.78	1.00
Aspect	Flat	82,385	4.30	0	0.00	0.00	0.00
	North	226,606	11.82	18	5.34	0.45	0.25
	Northeast	292,155	15.24	39	11.57	0.76	0.42
	East	299,541	15.62	56	16.62	1.06	0.58
	Southeast	247,143	12.89	33	9.79	0.76	0.42
	South	165,431	8.63	53	15.73	1.82	1.00
	Southwest	169,659	8.85	35	10.39	1.17	0.64
	West	209,333	10.92	57	16.91	1.55	0.85
	Northwest	225,221	11.75	46	13.65	1.16	0.64
Curvature	Concave	557,948	29.10	99	29.38	1.01	0.44
	Flat	785,003	40.94	91	27.00	0.66	0.00
	Convex	574,523	29.96	147	43.62	1.46	1.00
Distance from drainage	Buffer (100 m)	1,421,849	74.15	243	72.11	0.97	0.85
	Buffer (200 m)	374,666	19.54	74	21.96	1.12	0.98
	Buffer (300 m)	86,849	4.53	14	4.15	0.92	0.80
	Buffer (400 m)	29,718	1.55	6	1.78	1.15	1.00
	Buffer (>400 m)	4,392	0.23	0	0.00	0.00	0.00
Distance from lineament	Buffer (100 m)	466,283	24.32	218	64.69	2.66	1.00
	Buffer (200 m)	425,867	22.21	88	26.11	1.18	0.44
	Buffer (300 m)	325,061	16.95	22	6.53	0.39	0.14
	Buffer (400 m)	242,507	12.65	8	2.37	0.19	0.07
	Buffer (500 m)	178,295	9.30	1	0.30	0.03	0.01
	Buffer (>500 m)	279,461	14.57	0	0.00	0.00	0.00
Soil texture	Sandy loam	915,636	47.75	227	67.36	1.41	0.65
	Fine sandy loam	8,648	0.45	0	0.00	0.00	0.00
	Gravelly sandy loam	2,625	0.14	1	0.30	2.17	1.00
	Loam	35,391	1.85	1	0.30	0.16	0.07
	Silt loam	32,060	1.67	0	0.00	0.00	0.00
	Gravelly loam	27,715	1.45	4	1.19	0.82	0.38
	Overflow area	43,180	2.25	2	0.59	0.26	0.12
	Rocky sandy	627,654	32.73	91	27.00	0.82	0.38
	Rocky loam	224,294	11.70	11	3.26	0.28	0.13
	Gravelly sandy	271	0.01	0	0.00	0.00	0.00
Forest type	Nonforest	432,325	22.55	106	31.45	1.40	0.47
	Borad leaf tree	35,851	1.87	8	2.37	1.27	0.43
	Pine	1,036,557	54.06	175	51.93	0.96	0.33
	Cultivated	61,071	3.18	10	2.97	0.93	0.32
	Paper pulp	564	0.03	0	0.00	0.00	0.00
	Artificial pine	13,488	0.70	7	2.08	2.95	1.00
	Larch	84,023	4.38	11	3.26	0.74	0.25
	Korea nut pine	154,180	8.04	15	4.45	0.55	0.19
	Artificial rigida pine	5,468	0.29	0	0.00	0.00	0.00
	Mixing tree	93,947	4.90	5	1.48	0.30	0.10
Land cover	No data	0	0.00	0	0.00	0.00	0.00
	Water	4,824	0.25	1	0.30	1.18	0.46
	Urban	40,134	2.09	18	5.34	2.55	1.00
	Forest	1,715,778	89.49	287	85.16	0.95	0.37
	Grass	45,504	2.37	6	1.78	0.75	0.29

Table 2 continued

Factor	Class	No. of pixels in domain	Percentage of domain	No. of landslide	Percentage of landslide	Frequency ratio	Fuzzy membership values
	Rice field	106,446	5.55	23	6.82	1.23	0.48
	Barren	4,680	0.24	2	0.59	2.43	0.95

Domain: pixels in study area, *domain* (%): (domain/total pixels in study area) × 100, *landslide*: number of landslide occurrences, *landslide* (%): (landslide/total number of landslide occurrences) × 100, *frequency ratio*: landslide (%)/domain (%), *fuzzy membership values*: normalized value of the frequency ratio

The landslide-susceptibility analysis results were verified using the existing landslide locations in the study area. The verification method was performed by comparison of existing landslide data and landslide-susceptibility analysis results for the study area. The comparison results are shown in Fig. 3 as a line graph, which illustrates how well the landslide susceptibility maps of nine cases match with respect to the landslides used in constructing those landslide susceptibility maps. To obtain the data for Fig. 3, relative ranks of landslide susceptibility map and landslide occurrence were compared for each case. For this aim, the probabilities were divided into classes of accumulated area ratio % (*x*-axis) according to the LSI value (*y*-axis).

For example, when applying fuzzy algebraic sum, the 90–100% (10%) class with the highest probability of a landslide contains 41% and the 80–100% class (20%) contains 59% of the landslides of study area. In the case of applying the fuzzy algebraic product, the 90–100% (10%) class with the highest probability of a landslide contains 58% and the 80–100% class (20%) contains 69% of the landslides of study area. In the case of the

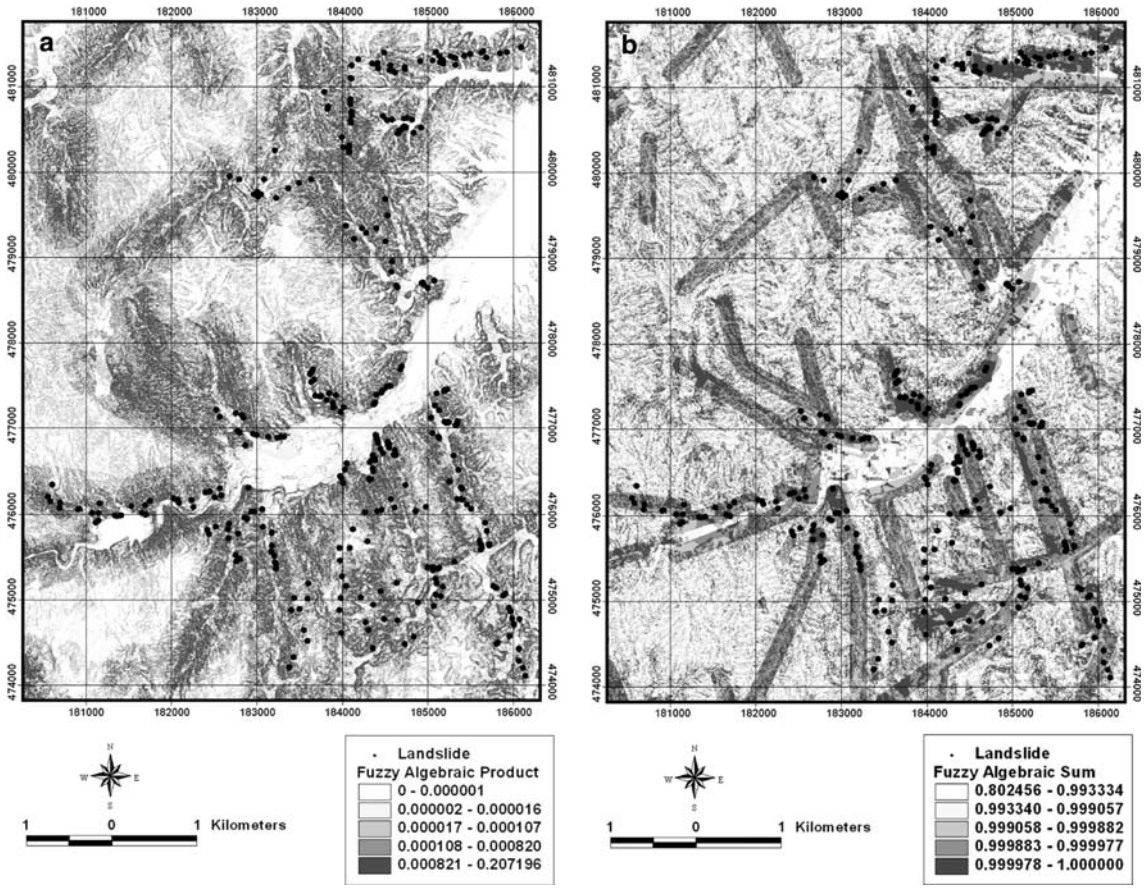

Fig. 2 Landslide susceptibility maps using various fuzzy operators. **a** Application of fuzzy algebraic product operator. **b** Application of fuzzy algebraic sum operator. **c** Application of fuzzy gamma ($\lambda = 0.025$) operator. **d** Application of fuzzy gamma ($\lambda = 0.5$) operator. **e** Application of fuzzy gamma ($\lambda = 0.975$) operator

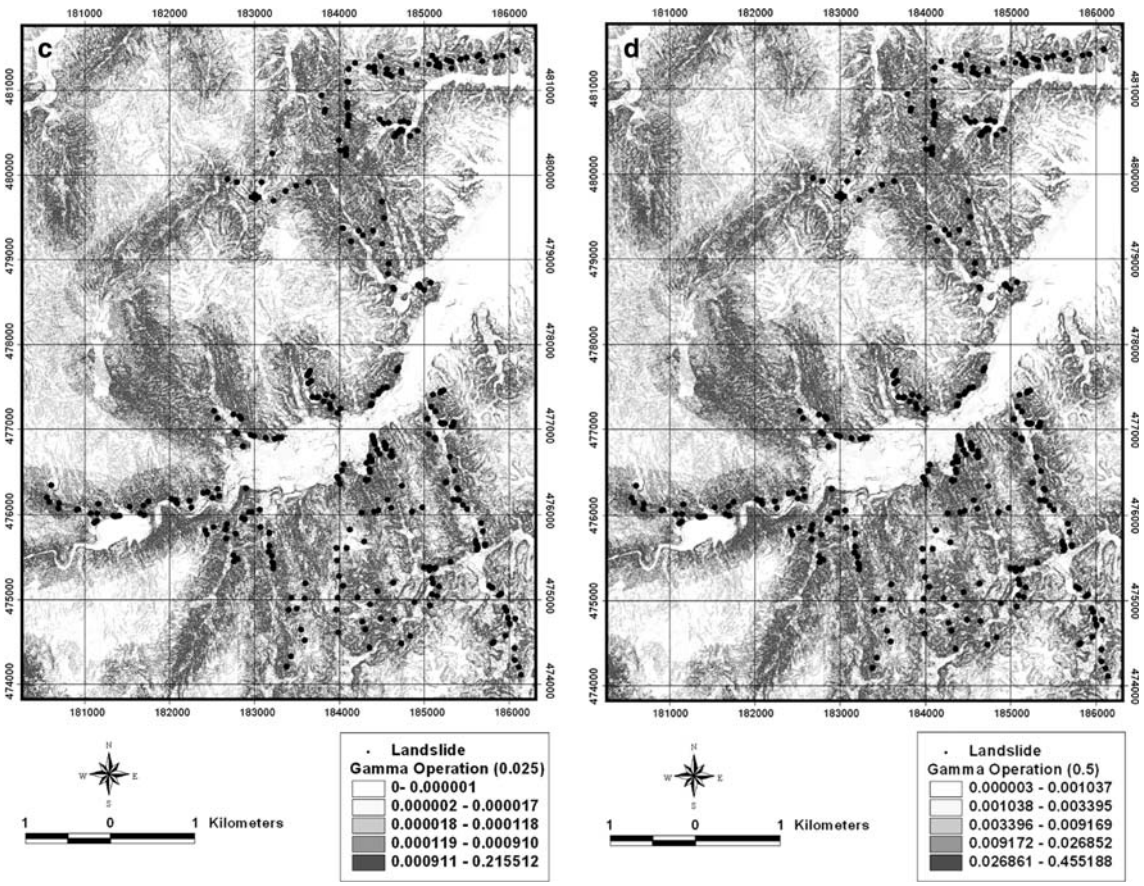

Fig. 2 continued

gamma operator ($\lambda = 0.975$), the 90–100% (10%) class with the highest possibility of a landslide contains 58% and the 80–100% class (20%) contains 69% of the landslides of study area. In the case of applying the gamma operator ($\lambda = 0.025$), the 90–100% (10%) class with the highest possibility of a landslide contains 58% and 80–100% class (20%) contains 69% of the landslides of study area.

To compare the results quantitatively, the areas under the curve were recalculated taking the total area as 1, which means perfect prediction accuracy. So, the area under a curve can be used to assess the prediction accuracy qualitatively for landslide susceptibility mapping. The area under the curve is shown in Table 3. For example, in the case of applying fuzzy algebraic sum, the area ratio was 0.7892 and we could say that the prediction accuracy is 78.92%. In the case of applying fuzzy algebraic product, the area ratio was 0.8458 and we could say that the prediction accuracy is 84.58%. In the case of applying the gamma operator ($\lambda = 0.975$), the area ratio was 0.8468 and the prediction accuracy is 84.68%.

Discussion and conclusions

Different fuzzy operators and different λ values for the gamma operation were tested on the input fuzzy membership functions to generate the most reliable landslide susceptibility map. The membership values assigned to each evidence map also play an important role in the final results. The fuzzy operators used in the first or further steps of analyses also affect the possibilities obtained in the final susceptibility map.

After verification, among the 17 cases, the case of applying the gamma operator ($\lambda = 0.975$), showed the best accuracy (84.68%), whereas the fuzzy and (66.79%) and fuzzy or (66.50%) operators showed the worst accuracy. In the case of applying the gamma operator with different λ value, the prediction accuracy had a similar value, between 84.55 and 84.68%. Generally, the verification results showed satisfactory agreement between the susceptibility map and the existing data from landslide locations. The effect of choosing different values of gamma (between 0 and 1) is not large. Because the landslide susceptibility maps

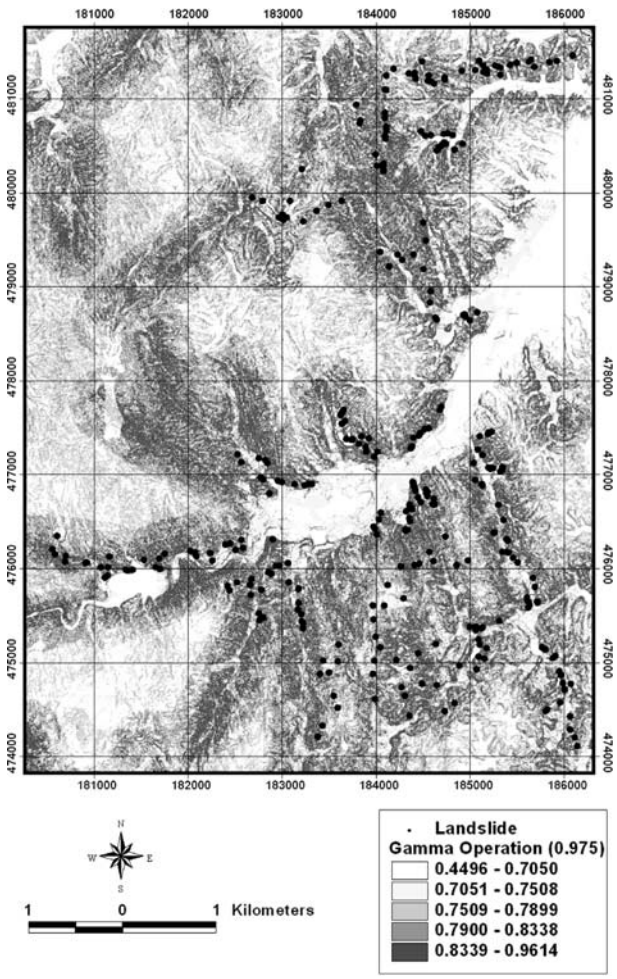

Fig. 2 continued

using different values of gamma (Fig. 2) are very similar and the prediction accuracy after verification is also very similar.

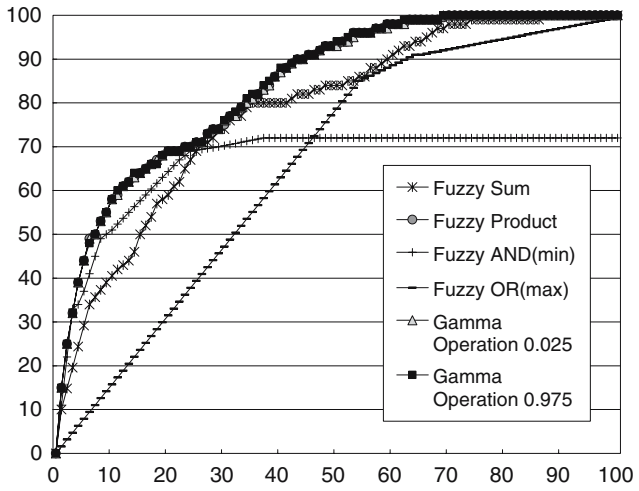

Fig. 3 Illustration of cumulative frequency diagram showing landslide susceptibility index rank (*x*-axis) occurring in cumulative percent of landslide occurrence (*y*-axis)

Table 3 Verification results using area under curve (AUC)

Fuzzy operator	Prediction accuracy (%)
Fuzzy and	66.79
Fuzzy or	66.50
Fuzzy algebraic sum	78.92
Fuzzy algebraic product	84.58
Gamma (λ) = 0.025	84.57
Gamma (λ) = 0.05	84.58
Gamma (λ) = 0.1	84.55
Gamma (λ) = 0.2	84.55
Gamma (λ) = 0.3	84.55
Gamma (λ) = 0.4	84.55
Gamma (λ) = 0.5	84.55
Gamma (λ) = 0.6	84.56
Gamma (λ) = 0.7	84.57
Gamma (λ) = 0.8	84.58
Gamma (λ) = 0.9	84.61
Gamma (λ) = 0.95	84.63
Gamma (λ) = 0.975	84.68

In the study, the data-derived model (frequency ratio) and the knowledge-derived model (fuzzy logic) were combined. As a result, the combined data and knowledge derived model is useful for landslide susceptibility mapping considering the prediction accuracy.

Acknowledgments This research was supported by the Basic Research Project of the Korea Institute of Geoscience and Mineral Resources (KIGAM) funded by the Ministry of Science and Technology of Korea.

References

Atkinson PM, Massari R (1998) Generalized linear modeling of susceptibility to landsliding in the central Apennines, Italy. Comput Geosci 24:373–385

Baeza C, Corominas J (2001) Assessment of shallow landslide susceptibility by means of multivariate statistical techniques. Earth Surf Process Landforms 26:251–1263

Bonham-Carter GF (1994) Geographic information systems for geoscientists, modeling with GIS. Pergamon, Oxford, 398 pp

Carro M, De Amicis M, Luzi L, Marzorati S (2003) The application of predictive modeling techniques to landslides induced by earthquakes: the case study of the 26 September 1997 Umbria-Marche earthquake (Italy). Eng Geol 69:139–159

Clerici A, Perego S, Tellini C, Vescovi P (2002) A procedure for landslide susceptibility zonation by the conditional analysis method. Geomorphology 48:349–364

Dai FC, Lee CF (2002) Landslide characteristics and slope instability modeling using GIS, Lantau Island, Hong Kong. Geomorphology 42:213–228

Dai FC, Lee CF, Li J, Xu ZW (2001) Assessment of landslide susceptibility on the natural terrain of Lantau Island, Hong Kong. Environ Geol 40:381–391

Donati L, Turrini MC (2002) An objective method to rank the importance of the factors predisposing to landslides with the GIS methodology: application to an area of the Apennines (Valnerina; Perugia, Italy). Eng Geol 63:277–289

Ercanoglu M, Gokceoglu C (2002) Assessment of landslide susceptibility for a landslide-prone area (north of Yenice, NW Turkye) by fuzzy approach. Environ Geol 41:720–730

Ercanoglu M, Gokceoglu C (2004) Use of fuzzy relations to produce landslide susceptibility map of a landslide prone area (West Black Sea Region, Turkey). Eng Geol 75:229–250

Gokceoglu C, Sonmez H, Ercanoglu M (2000) Discontinuity controlled probabilistic slope failure risk maps of the Altindag (settlement) region in Turkey. Eng Geol 55:277–296

Guzzetti F, Carrarra A, Cardinali M, Reichenbach P (1999) Landslide hazard evaluation: a review of current techniques and their application in a multi-scale study. Central Italy. Geomorphology 31:181–216

Jibson RW, Harp EL, John AM (2000) A method for producing digital probabilistic seismic landslide hazard maps. Eng Geol 58:271–289

Lee S (2004) Application of likelihood ratio and logistic regression model for landslide susceptibility mapping using GIS. Environ Manage 34:223–232

Lee S, Choi U (2003) Development of GIS-based geological hazard information system and its application for landslide analysis in Korea. Geosci J 7:243–252

Lee S, Choi J (2004) Application of a weight-of-evidence model to landslide susceptibility analysis. Int J Geogr Inf Sci 18:789–814

Lee S, Min K (2001) Statistical analysis of landslide susceptibility at Yongin, Korea. Environ Geol 40:1095–1113

Lee S, Chwae U, Min K (2002a) Landslide susceptibility mapping by correlation between topography and geological structure: the Janghung area, Korea. Geomorphology 46:49–162

Lee S, Choi J, Min K (2002b) Landslide susceptibility analysis and verification using the Bayesian probability model. Environ Geol 43:120–131

Lee S, Ryu JH, Min KD, Won JS (2003a) Landslide susceptibility analysis using GIS and artificial neural network. Earth Surf Process Landforms 27:1361–1376

Lee S, Ryu JH, Lee MJ, Won JS (2003b) Landslide susceptibility analysis using artificial neural network at Boun, Korea. Environ Geol 44:820–833

Lee S, Ryu JH, Won JS, Park HJ (2004a) Determination and application of the weights for landslide susceptibility mapping using an artificial neural network. Eng Geol 71:289–302

Lee S, Choi J, Woo I (2004b) The effect of spatial resolution on the accuracy of landslide susceptibility mapping: a case study in Boun, Korea. Geosci J 8:51–60

Lee S, Choi J, Min K (2004c) Landslide hazard mapping using GIS and remote sensing data at Boun, Korea. Int J Remote Sens 25:2037–2052

Luzi L, Pergalani F, Terlien MTJ (2000) Slope vulnerability to earthquakes at subregional scale, using probabilistic techniques and geographic information systems. Eng Geol 58:313–336

Ohlmacher GC, Davis JC (2003) Using multiple logistic regression and GIS technology to predict landslide hazard in northeast Kansas, USA. Eng Geol 69:331–343

Parise M, Jibson RW (2000) A seismic landslide susceptibility rating of geologic units based on analysis of characteristics of landslides triggered by the 17 January, 1994 Northridge, California earthquake. Eng Geol 58:251–270

Pistocchi A, Luzi L, Napolitano P (2002) The use of predictive modeling techniques for optimal exploitation of spatial databases: a case study in landslide hazard mapping with expert system-like methods. Environ Geol 41:765–775

Refice A, Capolongo D (2002) Probabilistic modeling of uncertainties in earthquake-induced landslide hazard assessment. Comput Geosci 28:735–749

Romeo R (2000) Seismically induced landslide displacements: a predictive model. Eng Geol 58:337–351

Shou KJ, Wang CF (2003) Analysis of the Chiufengershan landslide triggered by the 1999 Chi-Chi earthquake in Taiwan. Eng Geol 68:237–250

Zadeh LA (1965) Fuzzy sets. IEEE Inf Control 8:338–353

Zhou CH, Lee CF, Li J, Xu ZW (2002) On the spatial relationship between landslides and causative factors on Lantau Island, Hong Kong. Geomorphology 43:197–207

Zhou G, Esaki T, Mitani Y, Xie M, Mori J (2003) Spatial probabilistic modeling of slope failure using an integrated GIS Monte Carlo simulation approach. Eng Geol 68:373–386

Zimmerman HJ (1996) Fuzzy set theory and it applications. Kluwer, Massachusetts, 435 pp